JOC The Journal of Organic Chemistry

Article

pubs.acs.org/joc

Syntheses and Properties of Nine-Ring-Fused Linear Thienoacenes

Yu Xiong,† Xiaolan Qiao,† Hongzhuo Wu, Qiuliu Huang, Qinghe Wu, Jie Li, Xike Gao, and Hongxiang Li*

Shanghai Institute of Organic Chemistry, CAS, Shanghai 200032, China

Supporting Information

ABSTRACT: π-Extended nine-ring-fused linear thienoacenes **1a**–**c** with internal thieno[3,2-*b*;4,5-*b*′]dithiophene substructures were synthesized. Their optical and electrochemical properties were investigated. Thin-film transistor characteristics showed all compounds displayed high device reproducibility and nearly no dependence on substrate temperatures. The highest performance was observed for **1c**-based devices with mobility up to 1.0 cm^2/Vs and current on/off ratio of 10^7, whereas the maximum mobility was 0.5 cm^2/Vs for **1b** and 0.011 cm^2/Vs for **1a**.

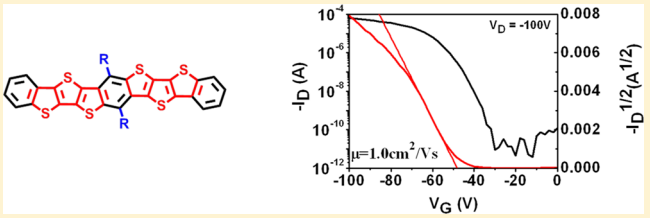

INTRODUCTION

Linear acenes (such as pentacene) are excellent organic semiconductors and usually display high thin-film transistor (TFT) performance due to their planar conjugated structures.[1−4] However, most of the linear acenes are not stable under ambient conditions because of their high-lying HOMO energy levels[1,5] and chemical reactivity.[6] The instability of linear acenes hinders their practical applications in TFTs.[7] Compared with acenes, linear thienoacenes exhibit not only high transistor performance but also excellent ambient stability.[8−13] For example, DNTT (chemical structure see Scheme 1) shows a hole mobility of 2.9 cm^2/Vs and is much more stable than pentacene and hexacene.[10c] The high performance and good stability of linear thienoacenes suggests their great potential applications to TFTs. However, due to the synthesis and purification difficulties, most of the reported linear thienoacenes are four- to seven-ring fused ones.[10,14−16] In order to explore new type of high-performance linear thienoacenes and investigate their structure−property relationships, it is important and desirable to synthesize thienoacenes with larger conjugation length.

Scheme 1. Some Representative Linear Thienoacenes

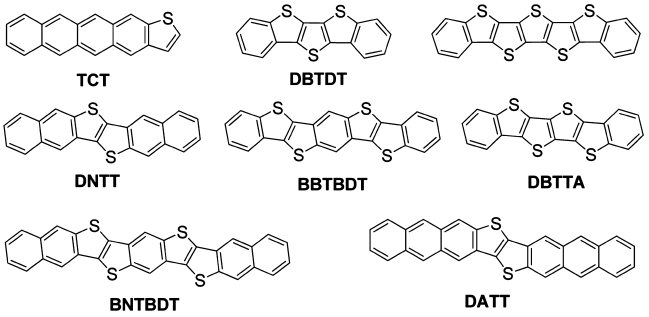

Currently, the common units in thienoacenes are thiophene and thieno[3,2-*b*]thiophene (TT) substructures (see Scheme 1).[5,8] Thienoacenes with higher conjugated thiophene substructures (such as thieno[3,2-b;4,5-*b*′]dithiophene (TDT) and thieno(2″,3″:4′,5′)thieno(2′,3′-d)thieno(3,2-b)thiophene (TTA)) are rare (for some examples, see Scheme 1).[11,17] We have reported that TDT-containing linear thienoacene DBTDT displayed excellent mobility (0.5 cm^2/Vs on thin-film transistors and 1.8 cm^2/Vs on single crystal transistors) and stability, suggesting TDT-containing thioacenes are good candidates for high-performance organic semiconductors.[11a,b] In order to further investigate the application of TDT contained linear thienoacenes in organic transistors and study the influence of the conjugation length to device performance, herein, nine-ring-fused thienoacenes, **1a**–**c** (for chemical structures, see Scheme 3) were designed and synthesized. These compounds possessed two TDT substructures and were substituted at the center phenyl ring with alkyl/alkyloxyl chains. The substituents will (i) increase the solubility of **1a**–**c**, which facilitates their purifications, and (ii) be helpful toward understanding the effect of substituents on device performance, which is one of the key challenges for the advances of OFETs.[10a,b,d,18] Thin-film transistor characteristics showed **1a**–**c** displayed high peformance (mobility >1.0 cm^2/Vs and current on/off ratio >10^7), high device reproducibility, and nearly no dependence on substrate temperatures. The physicochemical properties of **1a**–**c** were also investigated.

RESULTS AND DISCUSSION

The syntheses of **1a**–**c** were first attempted by lithiating of tetrabromo presursor **5**, followed by reaction with $(PhSO_2)_2S$, which has been successfully applied to the synthesis of DBTDT (Scheme 2).[11a] However, no target product was obtained. The

Received: November 21, 2013
Published: December 29, 2013

   dx.doi.org/10.1021/jo4025607 | J. Org. Chem. 2014, 79, 1138−1144

Scheme 2. Lithiation of Tetrabromo Precursor Method

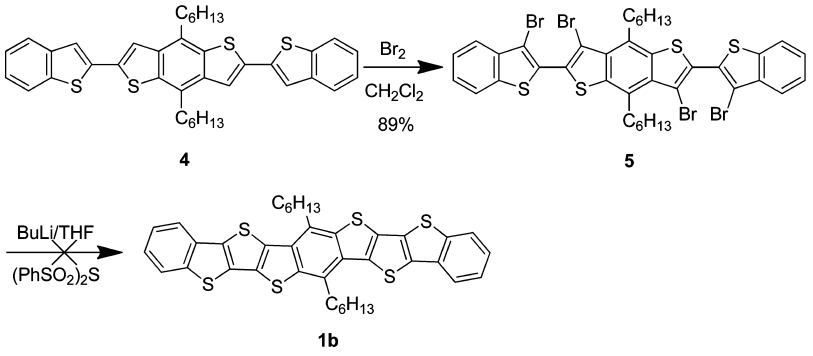

Scheme 3. Synthesis and Chemical Structures of 1a−c

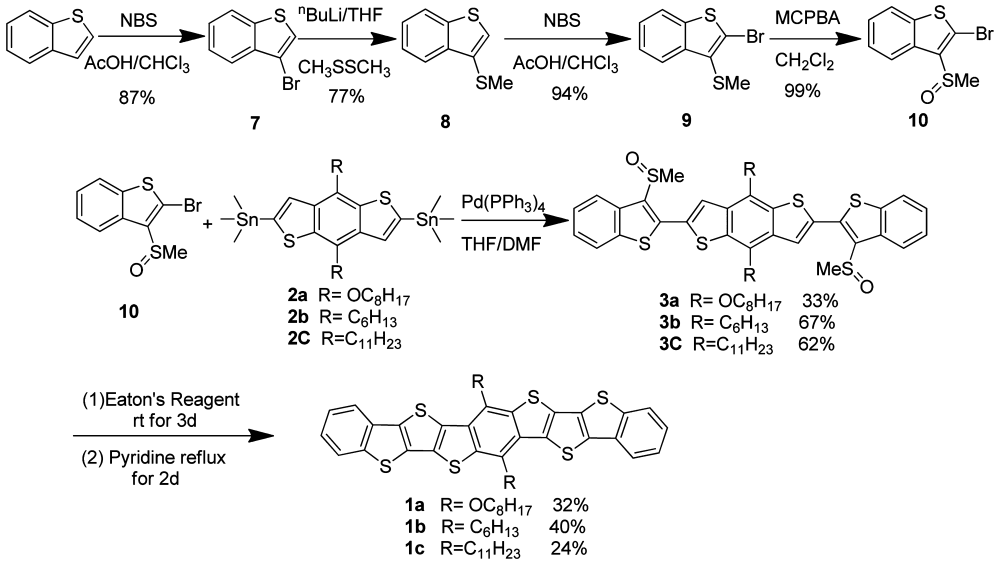

reason might be that the lithiation of four bromine atoms was difficult and complicated due to the poor solubility and/or instability of the lithiation intermediates. Thus, the dimethylsulfinyl ring-closing method was used (Scheme 3). This synthetic procedure includes two key steps: a Stille cross-coupling of dimethylsulfinyl benzothiophene with the 2,6-bis(trimethyltin)benzo[1,2-*b*;4,5-*b*′]dithiophene derivatives and a double intramolecular ring-closing reaction of the dimethylsulfinyl benzothiophene with the adjacent thiophenes. The coupling of dimethylsulfinyl benzothiophene **10** with the corresponding 2,6-bis(trimethyltin)benzo[1,2-*b*;4,5-*b*′]dithiophene derivatives **2** afforded compounds **3** in moderate isolated yields.[19,20] Because of the alkyl/alkyloxyl chains and the sulfinyl groups, compounds **3** have good solubility in organic solvents and could be easily purified by column chromatography. Initially, the intramolecular ring-closing reaction of the precursors **3** was induced by trifluoromethanesulfonic acid.[21] However, very complex products were obtained, which might be due to the strong acid property of trifluoromethanesulfonic acid. Thus, a relatively mild acid, Eaton's reagent (7.7 wt % P_2O_5 in CH_3SO_3H), was used to promote the intramolecular cyclization reaction.[22] Compounds **1a−c** were successfully prepared and precipitated from the reaction mixtures. Further purification by recrystallization from chlorobenzene solution afforded **1a−c** as yellow solids. Unfortunately, attempts to synthesize the unsubstituted nine-ring fused thienoacene by the dimethylsulfinyl ring-closing method failed. We believed the reason should be ascribed to the lower nucleophilic reactivity of nonalkyl/alkyloxyl-substituted benzo[1,2-*b*;4,5-*b*′]dithiophene. The solubilities of **1a−c** in organic solvents were much poorer compared with that of compounds **3**, which is caused by their rigid and large conjugated planar structures. They were fully characterized by ^{1}H NMR, MS, and elemental analyses (due to the low solubility, the ^{13}C NMR of **1a−c** could not be obtained).

The electrochemical properties of **1a−c** were examined by cyclic voltammetry (CV). The CVs of **1a** and **1c** were carried out in hot chlorobenzene solutions (SCE was used as reference electrode), whereas that of **1b** was conducted on thin film (Ag/$AgNO_3$ was used as reference electrode) owing to its poor solubility (see the Supporting Information, Figure S1). Their first oxidation potentials estimated from the midpoint of the peak potentials in the forward and backward scan were 0.91 V for **1a**, 0.86 V for **1b**, and 1.20 V for **1c**. The corresponding HOMO energy levels of **1a−c** calculated from CV curves were −5.22, −5.53, and −5.51 eV, respectively (the redox potential for ferrocene was 0.49 V vs SCE in solution and 0.13 V vs Ag/$AgNO_3$ in film). The higher HOMO energy level of **1a** is due to the stronger electron-donating ability of the side octyloxyl chain than that of hexyl and undecyl chains. The HOMO energy levels suggest these compounds are suitable as air-stable p-channel organic semiconductors.[23]

The absorption spectra of **1a−c** in solution and on thin film are illustrated in Figure 1. All compounds exhibited strong

dx.doi.org/10.1021/jo4025607 | *J. Org. Chem.* 2014, 79, 1138−1144

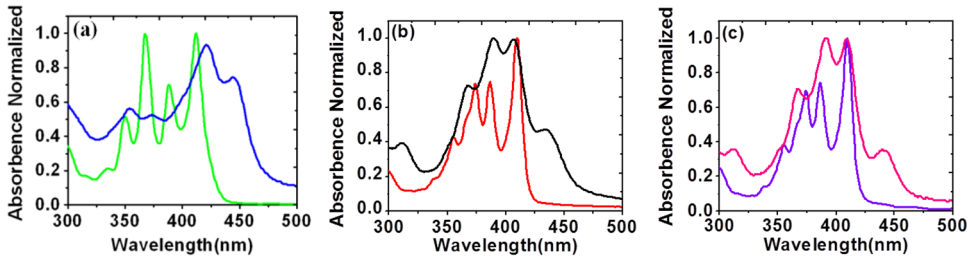

Figure 1. Absorption spectra of (a) **1a** (green line in CH_2Cl_2 solution/blue line on film); (b) **1b** (red line in CH_2Cl_2 solution/black line on film); (c) **1c** (violet line in CH_2Cl_2 solution/pink line on film).

absorptions in the region from 330 to 450 nm. For **1a**, the maximum peaks in the thin film were red-shifted (~10 nm) from that of solution, while **1b** exhibited a blue shift (~ 4 nm) and **1c** showed neither red shift nor blue shift. At the same time, new shoulder peaks at 445 nm for **1a**, 435 nm for **1b** and 440 nm for **1c** were observed on thin film spectra. The thin film absorption spectra suggested these compounds possessed strong intermolecular interactions and adopted different molecular packings in the solid state, which is further proved by the XRD results (vide infra). The optical energy bandgaps calculated from the onset absorptions in solution were 2.84 eV for **1a**, 2.92 eV for **1b**, and 2.90 eV for **1c**, indicating that the introduction of stronger electron-donating substituents slightly reduced the HOMO−LUMO energy gaps.

The charge-transport properties of **1a−c** were investigated by thin film transistors. The transistors were fabricated with top-contact/bottom-gate device configurations. The thin films were deposited in high vacuum onto octadecyltrichlorosilane (OTS)-modified Si/SiO_2 substrates. The Au source and drain electrodes were fabricated through a shadow mask by vacuum evaporation with a channel length of 273 μm and width of 31 μm. The mobility was extracted from the saturation regime. All of the compounds exhibited well-defined p-channel transistor response, and the typical output and transfer curves are given in Figure 2.

Table 1 summarizes the transistor performances of **1a−c** at different substrate temperatures (T_{sub}). Compounds **1b** and **1c** exhibited high transistor performance. The mobility was 0.27 cm^2/Vs for **1b** and 0.68 cm^2/Vs for **1c** when the T_{sub} was room temperature (25 °C). With the increase of the T_{sub}, the performance of **1b** and **1c** improved. For **1b**, the highest performance was observed at T_{sub} = 140 °C with mobility up to 0.5 cm^2/Vs and a high current on/off ratio of 10^7. Compound **1c** displayed the maximum mobility of 1.05 cm^2/Vs with a current on/off ratio of 10^7 at T_{sub} = 90 °C. The mobility of **1a** was 5×10^{-3} cm^2/Vs at T_{sub} = 25 °C (room temperature) and could reach 1.1×10^{-2} cm^2/Vs when T_{sub} was 140 °C. The performance of **1c** was about 1−2 orders of magnitude lower than that of **1b** and **1c**, regardless of the same surface treatment and optimized substrate temperature during deposition. This reveals the great effect of substituents on device performance. In addition, the output curve of **1a** showed prominent contact resistance compared with that of **1b** and **1c**, although the HOMO energy level of **1a** (−5.22 eV) matches the work function of the gold electrode better than that of **1b** and **1c** (−5.53 eV and −5.51 eV). This phenomenon might be attributed to the film disorder and/or a broader orientation distribution of **1a**, as shown in AFM and 2D-GIXD results.[24]

It is worth noting that most of the largely π-extended thienoacenes showed T_{sub}-dependent device performance. For example, BNTBDT (chemical structure see Scheme 1) displayed a mobility of more than 0.1 cm^2/Vs at T_{sub} higher than 100 °C, whereas the mobility was 10^{-3} cm^2/Vs at T_{sub} = 25 °C (room temperature).[15,25] Interestingly, the performance of **1a−c** did not exhibit obvious dependence on T_{sub}, which is beneficial for low-cost fabrication and flexible substrates. Moreover, the performance of **1b** and **1c** displayed good

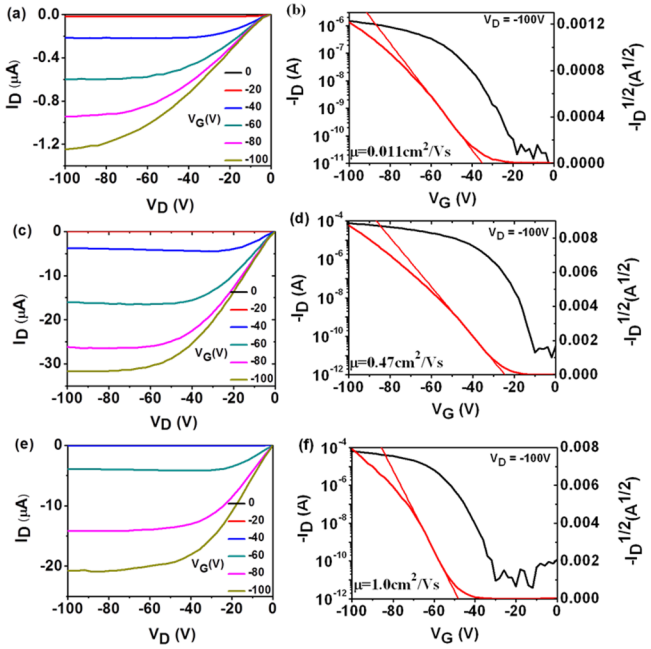

Figure 2. Typical output and transfer characteristics of **1a−c** based TFTs fabricated on OTS-treated Si/SiO_2 substrates: (a, b) **1a**; (c, d) **1b**; (e, f) **1c**.

Table 1. Electrical Characteristics of 1a−c Based Transistors Fabricated on OTS-Treated Si/SiO_2 Substrates under Different Substrate Temperatures

compd	T_{sub} (°C)	$\mu/cm^2/Vs$	V_{th} (V)	I_{on}/I_{off}
1a	rt	$4-5 \times 10^{-3}$	−16 to −21	10^3-10^4
	100	$8-8.9 \times 10^{-3}$	−23 to −31	~10^5
	140	$9-10 \times 10^{-3}$	−13 to −17	10^5-10^6
	160	$10-11 \times 10^{-3}$	−28 to −35	10^5-10^6
1b	RT	0.25−0.27	−25 to −30	10^6-10^7
	100	0.39−0.43	−17 to −23	10^6-10^7
	140	0.43−0.50	−25 to −32	10^6-10^7
	160	0.43−0.49	−35 to −39	10^6-10^7
1c	RT	0.53−0.68	−30 to −48	10^6-10^7
	90	0.8−1.05	−43 to −50	10^6-10^7
	150	0.51−0.53	−58 to −60	10^5-10^6

dx.doi.org/10.1021/jo4025607 | J. Org. Chem. 2014, 79, 1138−1144

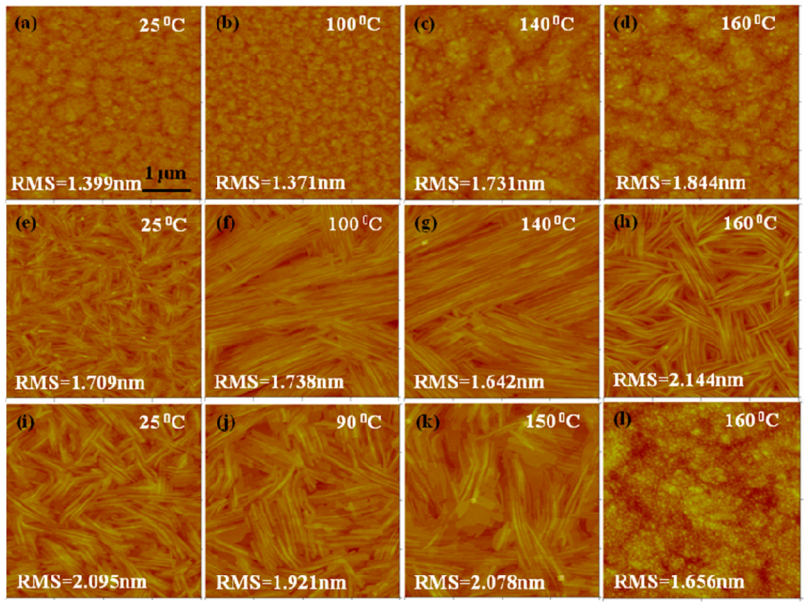

Figure 3. AFM images (a–k, 4 × 4 μm; l, 2 × 2 μm) of evaporated thin films for **1a–c** at various T_{sub} on OTS-treated substrates. (a–d) **1a**; (e–h) **1b**; (i–k) **1c**; (l) zoom image of (d).

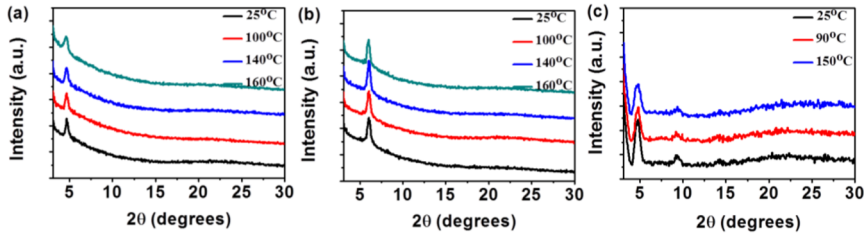

Figure 4. X-ray diffraction patterns of **1a–c** thin films on OTS-treated Si/SiO_2 substrates: (a) **1a**; (b) **1b**; (c) **1c**.

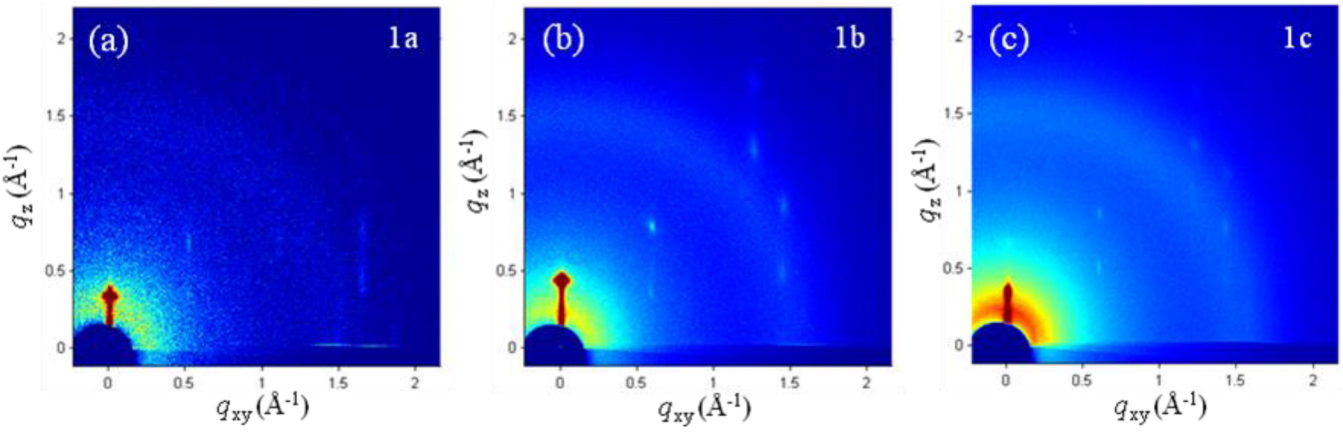

Figure 5. 2D-GIXD patterns for the thin films of (a) **1a** film grown at T_{sub} = 140 °C, (b) **1b** film grown at T_{sub} = 140 °C, (c) **1c** film grown at T_{sub} = 90 °C.

reproducibility at different substrate temperatures, which is crucial for the practical applications of TFTs.

In order to understand the performance difference of **1a–c**, their thin films were investigated by atomic force microscopy (AFM) and X-ray diffraction (XRD). AFM images showed all compounds formed continuous and smooth films, but their morphologies were different with the change of substituents (Figure 3). Fiber-like features with high order orientation existed in thin films of **1b** and **1c** (Figure 3e–k). Intriguingly, this kind of long-range order is different from that of other reported thienoacenes.[10c,11a,14] This is possibly caused by the substitution of the alkyl chains at the central phenyl ring. For **1b**, with the increase of T_{sub} (up to 140 °C), the size and the order of the fiber-like features were both increased. When T_{sub} was further increased to 160 °C, the domain size grew smaller and the coalescence became worse, agreeing well with the variation of the performance. For **1c** (Figure 3i–k), the domain size and orientations were inferior to that of **1b**. However, the adjacent domains coalesced well and lamella structures were observed in **1c** films. The higher the T_{sub}, the better of the film

dx.doi.org/10.1021/jo4025607 | J. Org. Chem. 2014, 79, 1138–1144

quality was for **1c**. This was incompatible with the deteriorated performance of **1c**-based devices at T_{sub} = 150 °C. The reason is still ambiguous and further detailed research is required to figure out the problem. Compared with that of **1b** and **1c**, the morphologies of **1a** consisted of disordered small-sized grains with high density grain boundaries (Figure 3a−d,l), which is in accordance with its low mobility and the relatively prominent contact resistance.

XRD results showed all compounds formed crystalline thin films, and the intensity of the diffraction peaks was almost independent of T_{sub} (Figure 4). The *d*-spacing estimated from XRD is 18.98 Å for **1a** (Figure 4a), 14.62 Å for **1b** (Figure 4b), and 18.57 Å for **1c** (Figure 4c). The *d*-spacing of **1a** and **1c** is very close to the length of conjugated backbone (18.998 Å) obtained by theoretical calculations (see the Supporting Information), indicating they are nearly perpendicular standing on the substrate. The *d*-spacing of **1b** is much shorter than the length of conjugated backbone, suggesting it is tilted or adopts different arrangement on the substrate. The different molecular arrangements and film morphologies should be responsible for the discrepancy of the device performances.

Because of the long side chains the attempt to grow single crystals of **1a−c** failed. Thin-film grazing incidence XRD (GIXRD) were further performed to study the film structure of **1a−c**. As shown in Figure 5, the rodlike (**1a**) and discrete (**1b** and **1c**) diffraction spots strongly suggested the high crystallinity of the films. The angular spread of the spectral peaks along q_z is related to the degree of the grain alignment to the substrate surface; a larger peak spread corresponds to a higher disorientation. The angular spread (fwhm) of peaks was 8.5° for **1a** at q_z∼0.33 Å^{-1}, 7.5° for **1b** at q_z∼ 0.43 Å^{-1} ,and 4.4° for **1c** at q_z∼0.34 Å^{-1}. It is well-known that the disorientation of the grains plays an important role to the OTFT performance.[26] Consequently, a higher mobility is expected for the **1c**-based device, consistent with the experiment results.

■ CONCLUSIONS

In summary, large π-extended thienoacenes **1a−c** were successfully synthesized and characterized. Experimental results showed all compounds had suitable HOMO energy levels as p-channel organic semiconductors for transistors. A high mobility up to 1.05 cm^2/Vs was observed for **1c**-based devices, whereas the mobility of **1a** and **1b** based transistors were 0.011 cm^2/Vs and 0.5 cm^2/Vs, respectively. Unlike most of the thienoacenes, compounds **1a−c** exhibited high device reproducibility and nearly no mobility/substrate temperature dependence, which is crucial for the practical applications of TFTs. AFM and XRD results suggested the different morphologies, and molecular packings in the films should be responsible for the performance variations of **1a−c**.

■ EXPERIMENTAL SECTION

All reactions were performed under an atmosphere of nitrogen unless stated otherwise. Tetrahydrofuran (THF) was distilled from sodium and benzophenone. *N*,*N*-Dimethylformamide (DMF) was purified by vacuum distillation. All chemicals were used directly without further purification unless otherwise noted. Compounds **2** were synthesized according to reported methods.[19,20]

3-Bromobenzo[*b*]thiophene (7). NBS (4.5 g, 25 mmol) was added in small portions to a solution of benzo[*b*]thiophene (2.7 g, 20 mmol) in 40 mL of $CHCl_3$/AcOH (1:1) under an ice−water bath. The reaction mixture was stirred at room temperature overnight before being poured into water. After extraction with CH_2Cl_2, the organic phase was separated and dried over anhydrous $MgSO_4$. The residue was purified by column chromatography (silica gel, eluent: petroleum) to obtain **7** as a colorless liquid 3.4 g (87%): ^{1}H NMR (300 MHz, $CDCl_3$, ppm) δ 7.88−7.86 (m, 2H), 7.52−7.41 (m, 3H); EI-MS *m*/*z* 214 (M$^+$, 100), 212 (M$^+$, 95.8).

3-Methylsulfenylbenzo[*b*]thiophene (8). A solution of 3-bromobenzo[*b*]thiophene **7** (1.1 g, 5 mmol) in tetrahydrofuran (10 mL) was cooled to −78 °C under nitrogen, and *n*-butyllithium (2.5 mL, 6 mmol) was added dropwise. After being stirred for 1 h at this temperature, the mixture was transferred via a cannula to an ice-cooled solution of methyl disulfide (1.2 g, 12.5 mmol) in tetrahydrofuran (8 mL), and the reaction mixture was warmed to room temperature and stirred overnight. Water was poured into the reaction mixture, and the organic phase was separated, washed with water, and dried over anhydrous $MgSO_4$. The residue was purified by column chromatography (silica gel, eluent: petroleum) to obtain **8** as a pale yellow liquid 3.9 g (77%): ^{1}H NMR (300 MHz, $CDCl_3$, ppm) δ 7.84 (t, 2H), 7.38 (m, 2H), 7.11 (s, 1H), 2.48 (s, 3H); EI-MS *m*/*z* 180 (M$^+$, 100).

2-Bromo-3-methylsulfenylbenzo[*b*]thiophene (9). NBS (2.4 g, 13.3 mmol) was added in small portions to a solution of 3-methylsulfinyl[b]thiophene **8** (2.0 g, 11.1 mmol) in 50 mL of AcOH under an ice−water bath. The reaction mixture was stirred at room temperature overnight before being poured into water. After extraction with CH_2Cl_2, the organic phase was separated and dried over anhydrous $MgSO_4$. The residue was purified by column chromatography (silica gel, eluent: petroleum) to obtain **9** as a pale yellow liquid 2.7 g (94%): ^{1}H NMR (300 MHz, $CDCl_3$, ppm) δ 7.94 (d, 1H), 7.74 (d, 1H), 7.46−7.34 (m, 2H), 2.38 (s, 3H); ^{13}C NMR (100 MHz, $CDCl_3$, ppm) δ 139.5, 139.2, 129.2, 128.8, 125.1, 123.3, 122.5, 121.9, 18.2; EI-MS *m*/*z* 258 (M$^+$, 100), 256 (M$^+$, 98.9); HR-MS (EI-MS) *m*/*z* 257.9177, calcd for ($C_9H_7S_2Br$) 257.9173.

2-Bromo-3-methylsulfinylbenzo[*b*]thiophene (10). To a solution of 2-bromo-3-methylsulfinyl[*b*]thiophene **9** (1.4 g, 5.4 mmol) in 20 mL of CH_2Cl_2 at 0 °C was added 3-chloroperbenzoic acid (1.3 g, 5.6 mmol, 75%) portionwise. The resulting solution was allowed to stir at room temperature overnight. The reaction mixture was washed with aqueous Na_2CO_3, dried ($MgSO_4$), and concentrated in vacuum to give 10 as white solid 1.5 g (99%): ^{1}H NMR (300 MHz, $CDCl_3$, ppm) δ 8.59 (dd, 1H), 7.79 (dd, 1H), 7.45−7.42 (m, 2H), 3.06 (s, 3H); EI-MS *m*/*z* 276 (M$^+$, 43.8), 274 (M$^+$, 40.8).

2,6-Bis(3-methylsulfinylbenzo[*b*]thiophene)-4,8-bis(hexyl)-benzo[1,2-*b*;4,5-*b*′]dithiophene (3b). A 50 mL Schlenk tube was charged with compound **10** (550 mg, 2 mmol), 2,6-bis (trimethyltin)-4,8-bis(hexyl)benzo[1,2-*b*;4,5-*b*′]dithiophene (684 mg, 1.0 mmol), and $Pd(PPh_3)_4$ (115 mg, 0.1 mmol). The mixture was degassed under high vacuum with a nitrogen purge. DMF/TFH (1:1) (20 mL) was successively injected into above system. The mixture was stirred overnight at 80 °C. After being cooled to room temperature, the mixture was poured into water and washed with ethyl acetate. The combined organic phase was dried over $MgSO_4$, and the residue was purified by column chromatography (silica gel, eluent: petroleum/tetrahydrofuran, 3/1, v/v) to afford **3b** as a yellow solid 490 mg (yield 33%): ^{1}H NMR (300 MHz, $CDCl_3$, ppm) δ 8.73 (d, 2H), 7.88 (d, 2H), 7.74 (s, 2H), 7.48 (m, 4H), 3.19 (m, 10H), 1.85 (m, 4H), 1.52 (m, 4H), 1.38 (m, 8H), 0.92 (t, 6H); ^{13}C NMR (100 MHz, $CDCl_3$, ppm) δ 139.1, 136.7, 136.5, 133.1, 132.3, 129.9, 129.8, 129.1, 126.1, 125.5, 124.5, 124.0, 122.4, 40.4, 33.2, 31.3, 29.7, 29.6, 22.7, 14.2; MS (MALDI-TOF) *m*/*z* 769 (M + Na$^+$, 21); HR-MS(MALDI-MS) *m*/*z* 769.1407, calcd for ($C_{40}H_{42}O_2S_6Na^{1+}$) 769.14013.

2,6-Bis(3-methylsulfinylbenzo[*b*]thiophene)-4,8-bis-(undecyl)benzo[1,2-*b*;4,5-*b*′]dithiophene (3c). Compound **3c** was synthesized according to a similar procedure for compound **3b**: yield 67%; ^{1}H NMR (300 MHz, $CDCl_3$, ppm) δ 8.72 (d, 2H), 7.85 (d, 2H), 7.72 (d, 2H), 7.46 (m, 4H), 3.17 (m, 10H), 1.84 (m, 4H), 1.49 (m, 4H), 1.39 (m, 4H), 1.25 (m, 24H), 0.85 (t, 6H); ^{13}C NMR (100 MHz, $CDCl_3$, ppm) δ 139.1, 139.1, 139.0, 136.7, 136.5, 133.1, 132.3, 129.9, 126.1, 125.5, 124.5, 123.9, 122.4, 40.2, 33.3, 31.9, 29.9, 29.7, 29.7, 29.6, 29.6, 29.5, 29.4, 22.7, 13.9; MS (MALDI-TOF) *m*/*z* 887 (M+H$^+$, 100); HR-MS(MALDI-MS) *m*/*z* 909.2983, calcd for ($C_{50}H_{62}O_2S_6Na^{1+}$) 909.29663.

dx.doi.org/10.1021/jo4025607 | J. Org. Chem. 2014, 79, 1138−1144

2,6-Bis(3-methylsulfinylbenzo[*b*]thiophene)-4,8-bis-(octaxyloxy)benzo[1,2-*b*;4,5-*b*′]dithiophene (3a). Compound **3a** was synthesized according to a similar procedure for compound **3b**: yield 62%; ^{1}H NMR (300 MHz, $CDCl_3$, ppm) δ 8.72 (m, 2H), 7.90 (m, 2H), 7.74 (s, 2H), 7.50 (m, 4H), 4.35 (t, 4H), 3.20 (s, 6H), 1.93 (m, 4H), 1.67 (m, 4H), 1.33 (m, 16H), 0.89 (t, 6H); ^{13}C NMR (100 MHz, $CDCl_3$, ppm) δ 144.7, 139.2, 138.6, 136.7, 133.2, 132.2, 131.1, 128.9, 126.3, 125.6, 124.1, 122.9, 122.5, 74.5, 40.4, 31.9, 30.6, 29.5, 29.4, 26.2, 22.7, 14.2; MS (MALDI-TOF) *m*/*z* 834 (M^+, 100); HR-MS (MALDI-MS) *m*/*z* 834.2030, calcd for ($C_{44}H_{50}O_4S_6^{1+}$) 834.20279.

General Procedures for the Syntheses of 1a–c. ***1a***. Compound **3a** (510 mg, 0.6 mmol) was stirred with Eaton's reagent (6 mL) at room temperature in the dark for 3 days. The mixture was poured into ice–water, and the brown solid collected by suction–filtration was dried in vacuum. The solid was transferred to a dry 100 mL three-neck flask, and pyridine (100 mL) was added. The mixture was refluxed for 1 day. After the mixture was cooled to room temperature, the precipitate was collected by suction–filtration and washed with CH_2Cl_2 and acetone successively. Finally, recrystallization from $CHCl_3$ and chlorobenzene in succession gave **1a** as a yellow solid (150 mg, 32%): mp 226 °C; ^{1}H NMR (400 MHz, $CDCl_2CDCl_2$ (100 °C), ppm) δ 7.83 (t, 4H), 7.38 (t, 2H), 7.30 (t, 2H), 4.41 (t, 4H), 2.05 (q, 4H), 1.62 (q, 4H), 1.44 (q, 4H), 1.29–1.38 (m, 12H), 0.85 (t, 6H); MS (MALDI-TOF) *m*/*z* 770 (M^+, 100). Anal. Calcd for $C_{42}H_{42}O_2S_6$: C, 65.41; H, 5.49. Found: C, 65.29; H, 5.35.

1b. Recrystallization from chlorobenzene several times gave yellow crystals (270 mg, 40%): mp 335 °C; ^{1}H NMR (400 MHz, $CDCl_2CDCl_2$ (100 °C), ppm) δ 7.82 (t, 4H), 7.37 (t, 2H), 7.29 (t, 2H), 3.28 (t, 4H), 1.90 (q, 4H), 1.64 (q, 4H), 1.39 (m, 8H), 0.89 (t, 6H); MS (MALDI-TOF) *m*/*z* 682 (M^+, 100). Anal. Calcd for $C_{38}H_{34}S_6$: C, 66.82; H, 5.02. Found: C, 66.77; H, 5.03.

1c. Recrystallization from chlorobenzene several times gave yellow crystals (120 mg, 24%): mp 260 °C; ^{1}H NMR (400 MHz, $CDCl_2CDCl_2$ (100 °C), ppm) δ 7.77 (dd, 4H), 7.32 (t, 2H), 7.24 (t, 2H), 3.23 (t, 4H), 1.87 (q, 4H), 1.61 (q, 4H), 1.41 (q, 4H), 1.27 (m, 24H), 0.80 (t, 6H); MS (MALDI-TOF) *m*/*z* 821 ($M-H^+$, 100); HR-MS(MALDI-MS) *m*/*z* 822.254 calcd for ($C_{48}H_{54}S_6^{1+}$) 822.25443. Anal. Calcd for $C_{48}H_{54}S_6$: C, 70.02; H, 6.61. Found: C, 69.77; H, 6.55.

2,6-Bis(benzo[*b*]thiophene)-4,8-bis(hexyl)benzo[1,2-*b*;4,5-*b*′]dithiophene(4). A 25 mL Schlenk tube was charged with 2-iodobenzo[*b*]thiophene (520 mg, 2 mmol), 2,6-bis(trimethyltin)-4,8-bis(hexyl)benzo[1,2-*b*;4,5-*b*′]dithiophene (684 mg, 1.0 mmol), and $Pd(PPh_3)_4$ (115 mg, 0.1 mmol). The mixture was purged under nitrogen atmosphere, and 10 mL of DMF was injected. The mixture was stirred overnight at 80 °C. After being cooled to room temperature, the mixture was poured into water and extracted with CH_2Cl_2. The combined organic phase was dried over $MgSO_4$, and the residue was purified by recrystallization from CH_3Cl to obtain **4** as a yellow solid 450 mg (yield 72%): ^{1}H NMR (400 MHz, $CDCl_2CDCl_2$(100 °C), ppm) δ 7.73 (dd, 4H), 7.69 (d, 2H), 7.53 (s, 2H), 7.48 (s, 2H), 7.27 (t, 4H), 3.10 (t, 4H), 1.52 (m, 4H), 1.47 (m, 4H), 1.33 (m, 8H), 0.86 (t, 6H); MS (MALDI-TOF) *m*/*z* 622 (M^+, 100); HR-MS(MALDI-MS) *m*/*z* 622.1854, calcd for ($C_{38}H_{38}S_4^{1+}$) 622.18509.

2,6-Bis(3-bromobenzo[*b*]thiophene)-3,7-dibromo-4,8-bis-(hexyl)benzo[1,2-*b*;4,5-*b*′]dithiophene (5). A 250 mL flask was charged with compound **4** (312 mg, 0.5 mmol) and 150 mL of CH_2Cl_2 under N_2. Br_2 (320 mg, 2 mmol) in 10 mL of CH_2Cl_2 was added dropwise at 0 °C. The reaction mixture was warmed to room temperature and stirred overnight. The mixture was treated with saturated $Na_2S_2O_3$ aqueous solution and extracted with $CHCl_3$. The organic phase was concentrated under vacuum evaporation, and the precipitate was filtered and washed of acetone and CH_2Cl_2 successively to obtain **5** as a yellow solid (yield, 420 mg. 89%): ^{1}H NMR (300 MHz, $CDCl_3$, ppm) δ 7.92 (dd, 2H), 7.85(dd, 2H), 7.50 (m, 4H), 3.60 (t, 4H), 1.87 (m, 4H), 1.55(m, 4H), 1.36 (m, 8H), 0.89 (t, 6H); ^{13}C NMR (100 MHz, $CDCl_3$, ppm) δ 139.7, 139.3, 138.0, 131.3, 131.2, 130.2, 126.3, 125.4, 124.0, 122.3, 111.4, 108.9, 31.5, 31.4, 30.9, 29.6, 22.6, 14.1; MS (MALDI-TOF) *m*/*z* 938 (M^+); HR-MS (MALDI-MS) *m*/*z* 855.9158 (M-Br) calcd for ($C_{38}H_{35}S_4Br_3^{1+}$) 855.91662.

Device Fabrication. The Si/SiO_2 substrates were cleaned and modified with octadecyltrichlorosilane (OTS) according to the reported procedure.[27] Transistor devices were fabricated in the top-contact bottom-gate device configurations. Thin films were deposited in high vacuum under different substrate temperatures to a thickness of 65 nm. The Au source and drain electrodes were deposited through a shadow mask by vacuum evaporation with a channle length 273 μm and width 31 μm.

■ ASSOCIATED CONTENT

Ⓢ Supporting Information

Cyclic voltammograms, emission spectra, and characterization data of all new compounds. This material is available free of charge via the Internet at http://pubs.acs.org.

■ AUTHOR INFORMATION

Corresponding Author

*E-mail: lhx@mail.sioc.ac.cn.

Author Contributions

†Y.X and X.Q. contributed equally.

Notes

The authors declare no competing financial interest.

■ ACKNOWLEDGMENTS

This work was financially supported by the National Natural Sciences Foundation of China (21190031, 51303201) and the National Basic Research Program of China (2011CB808405).

■ REFERENCES

(1) Mei, J.; Diao, Y.; Anthony, L. A.; Fang, L.; Bao, Z. *J. Am. Chem. Soc.* **2013**, *135*, 6724–6746.

(2) Wang, C.; Dong, H.; Hu, W.; Liu, Y.; Zhu, D. *Chem. Rev.* **2012**, *112*, 2208–2267.

(3) (a) Lee, S.; Koo, B.; Shin, J.; Lee, E.; Park, H.; Kim, H. *Appl. Phys. Lett.* **2006**, *88*, 162109. (b) Jurchescu, O. D.; Popinciuc, M.; van Wees, B. J.; Palstra, T. T. M. *Adv. Mater.* **2007**, *19*, 688–692.

(4) (a) Aleshin, A. N.; Lee, J. Y.; Chu, S. W.; Kim, J. S.; Park, Y. W. *Appl. Phys. Lett.* **2004**, *84*, 5383–5385. (b) De Boer, R. W.; Klapwijk, T. M.; Morpurgo, A. F. *Appl. Phys. Lett.* **2003**, *83*, 4345–4347. (c) Watanabe, M.; Chang, Y. J.; Liu, S.-W.; Chao, T.-H.; Goto, K.; IslamMd, M.; Yuan, C.-H.; Tao, Y.-T.; Shinmyozu, T.; Chow, T. J. *Nat. Chem.* **2012**, *4*, 574–578.

(5) Jiang, W.; Li, Y.; Wang, Z. *Chem. Soc. Rev.* **2013**, *42*, 6113–6127.

(6) Maliakal, A.; Raghavachari, K.; Katz, H.; Chandross, E.; Siegrist, T. *Chem. Mater.* **2004**, *16*, 4980–4986.

(7) (a) Mondal, R.; Shah, B. K.; Neckers, D. C. *J. Am. Chem. Soc.* **2006**, *128*, 9612–9613. (b) Anthony, J. E. *Angew. Chem., Int. Ed.* **2008**, *47*, 452–483. (c) Tang, M. L.; Bao, Z. *Chem. Mater.* **2011**, *23*, 446–455.

(8) Takimiya, K.; Shinamura, S.; Osaka, I.; Miyazaki, E. *Adv. Mater.* **2011**, *23*, 4347.

(9) Anthony, J. E. *Chem. Rev.* **2006**, *106*, 5028–5048.

(10) (a) Ebata, H.; Izawa, T.; Miyazaki, E.; Takimiya, K.; Ikeda, M.; Kuwabara, H.; Yui, T. *J. Am. Chem. Soc.* **2007**, *129*, 15732–15733. (b) Izawa, T.; Miyazaki, E.; Takimiya, K. *Adv. Mater.* **2008**, *20*, 3388. (c) Yamamoto, T.; Takimiya, K. *J. Am. Chem. Soc.* **2007**, *129*, 2224–2225. (d) Nakaama, K.; Hirose, Y.; Soeda, J.; Yoshizumi, M.; Uemura, T.; Uno, M.; Li, W.; Kang, M. J.; Yamagishi, M.; Okada, Y.; Miyazaki, E.; Nakaawa, Y.; Nakao, A.; Takimia, K.; Takeya, J. *Adv. Mater.* **2011**, *23*, 1626. (e) Kang, M. J.; Doi, I.; Mori, H.; Miyazaki, E.; Takimia, K.; Ikeda, M.; Kuwabara, H. *Adv. Mater.* **2011**, *23*, 1222. (f) Sokolov, A. N.; Atahan-Evrenk, S.; Mondal, R.; Akkerman, H. B.; Sanchez-Carrera, R. S.; Granados-Focil, S.; Schrier, J.; Mannsfeld, S. C. B.; Zoombelt, A. P.; Bao, Z.; Aspuru-Guzik, A. *Nat. Commun.* **2011**, *2*, 437. (g) Niimi,

K.; Shinamura, S.; Osaka, I.; Miyazaki, E.; Takimiya, K. *J. Am. Chem. Soc.* **2011**, *133*, 8732−8739.
(11) (a) Gao, J.; Li, R.; Li, L.; Meng, Q.; Jiang, H.; Li, H.; Hu, W. *Adv. Mater.* **2007**, *19*, 3008−3011. (b) Li, R.; Jiang, L.; Meng, Q.; Gao, J.; Li, H.; Tang, Q.; He, M.; Hu, W.; Liu, Y.; Zhu, D. *Adv. Mater.* **2009**, *21*, 4492. (c) Yasuo, M.; Eiji, Y.; Takeo, M.; Kazuhito, T.; Shigehiro, Y. *J. Mater. Chem.* **2012**, *22*, 7715.
(12) (a) Tang, M. L.; Okamoto, T.; Bao, Z. *J. Am. Chem. Soc.* **2006**, *128*, 16002. (b) Tang, M. L.; Mannsfeld, S. C. B.; Sun, Y. S.; Becerril, H. A.; Bao, Z. J. *Am. Chem. Soc.* **2009**, *131*, 882−883.
(13) (a) Zhou, Y.; Liu, W.; Ma, Y.; Wang, H.; Qi, L.; Cao, Y.; Wang, J.; Pei, J. *J. Am. Chem. Soc.* **2007**, *129*, 12386−12387. (b) Liu, W.; Zhou, Y.; Ma, Y.; Cao, Y.; Wang, J.; Pei, J. *Org. Lett.* **2007**, *9*, 4187−4190.
(14) Niimi, K.; Kang, M. J.; Miyazaki, E.; Osaka, I.; Takimiya, K. *Org. Lett.* **2011**, *13*, 3430−3433.
(15) Yamamoto, T.; Nishimura, T.; Mori, T.; Miyazaki, E.; Osaka, I.; Takimiya, K. *Org. Lett.* **2012**, *14*, 4914−4917.
(16) Mori, T.; Nishimura, T.; Yamamoto, T.; Doi, I.; Miyazaki, E.; Osaka, I.; Takimiya, K. *J. Am. Chem. Soc.* **2013**, *135*, 13900−13913.
(17) Huang, J.; Luo, H.; Wang, L.; Guo, Y.; Zhang, W.; Chen, H.; Zhu, M.; Liu, Y.; Yu, G. *Org. Lett.* **2012**, *14*, 3300−3303.
(18) Izawa, T.; Miyazaki, E.; Takimiya, K. *Chem. Mater.* **2009**, *21*, 903.
(19) Hu, X.; Shi, M.; Chen, J.; Zuo, L.; Fu, L.; Li, Y.; Chen, H. *Macromol. Rapid Commun.* **2011**, *32*, 506−511.
(20) Pan, H.; Li, Y.; Wu, Y.; Liu, P.; Beng, S.; Zhu, S.; Xu, G. *Chem. Mater.* **2006**, *18*, 3237−3241.
(21) Gao, P.; Beckmann, D.; Tsao, H. N.; Feng, X.; Enkelmann, V.; Baumgarten, M.; Pisula, W.; Müllen, K. *Adv, Mater.* **2009**, *21*, 213−216.
(22) Kim, J.; Han, A. R.; Seo, J. H.; Oh, J. H.; Yang, C. *Chem. Mater.* **2012**, *24*, 3464−3472.
(23) (a) Amanda, R. M.; Jean, M. J. F. *Chem. Rev.* **2007**, *107*, 1066−1096. (b) Locklin, J.; Ling, M. M.; Sung, A.; Roberts, M . E.; Bao, Z. *Adv. Mater.* **2006**, *18*, 2989.
(24) Guo, X.; Puniredd, S. R.; Baumgarten, M.; Pisula, W.; Müllen, K. *Adv, Mater.* **2013**, *25*, 5467−5472.
(25) (a) Liu, Y.; Wang, Y.; Wu, W.; Liu, Y.; Xi, H.; Wang, L.; Qiu, W.; Lu, K.; Du, C.; Yu, G. *Adv. Funct. Mater.* **2009**, *19*, 772−778. (b) Valiyev, F.; Hu, W.; Chen, H.; Kuo, M.; Chao, I.; Tao, Y. *Chem. Mater.* **2007**, *19*, 3018−3026.
(26) Rivnay, J.; Mannsfeld, S. C. B.; Miller, C. E.; Salleo, A.; Toney, M. F. *Chem. Rev.* **2012**, *112*, 5488−5519.
(27) Wang, M.; Li, J.; Zhao, G.; Wu, Q.; Huang, Y.; Hu, W.; Gao, X.; Li, H.; Zhu, D. *Adv. Mater.* **2013**, *25*, 2229−2233.